SECRET [redacted]

[redacted]

FEASIBILITY STUDY FINAL REPORT

GEODETIC ORBITAL PHOTOGRAPHIC SATELLITE SYSTEM

VOLUME 2 DATA COLLECTION SYSTEMS

JUNE 1966

SECRET [redacted]

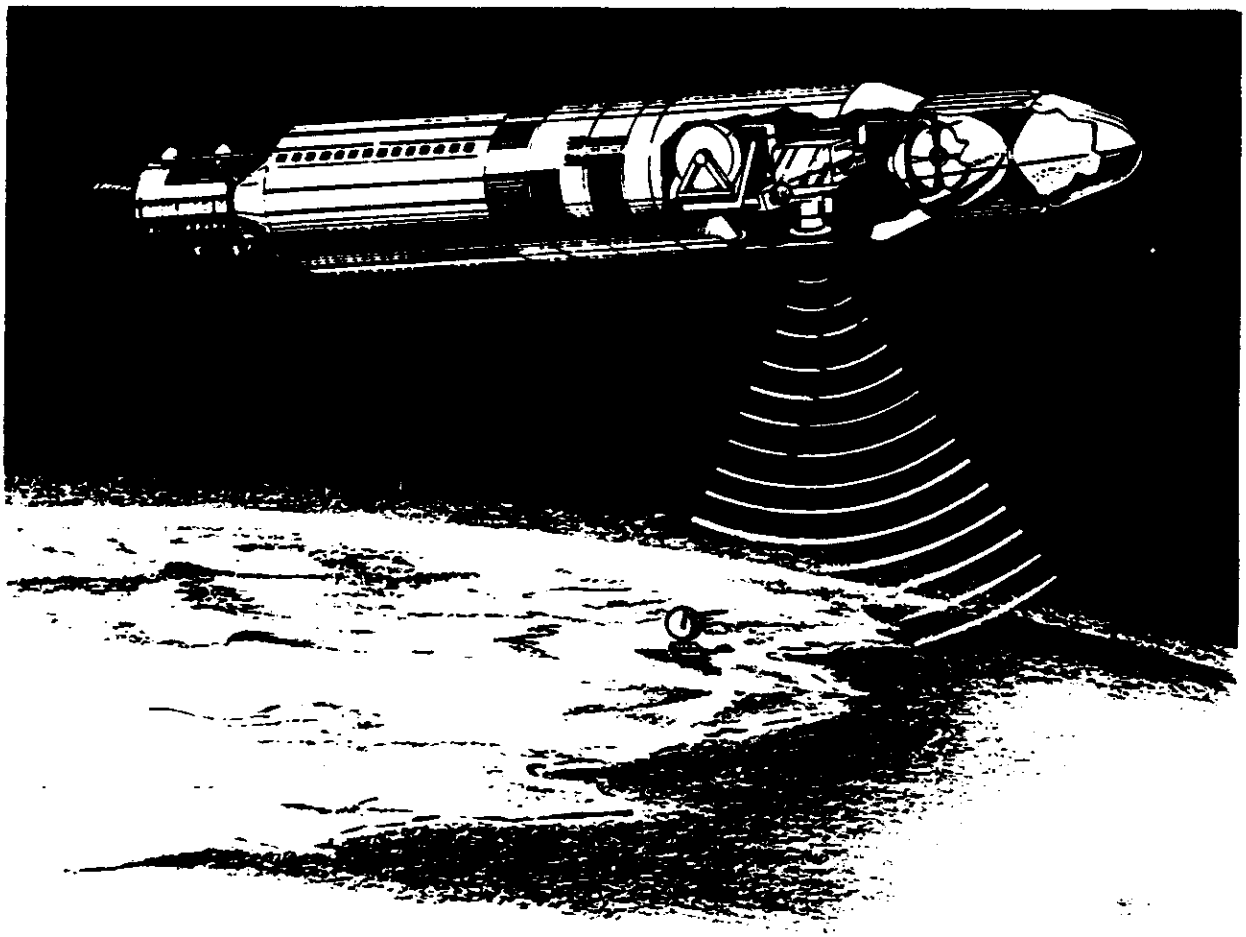

Geodetic Orbital Photographic Satellite System

CONTENTS

FIGURES

TABLES

PREFACE

The objective of the Geodetic Orbital Photographic Satellite System (GOPSS) is to accurately determine the location of landmarks widely distributed over the earth's surface and provide better information concerning the geophysical parameters which affect this system and other systems operating at similar altitudes. The means chosen to accomplish this objective is to orbit a series of data acquisition systems supported by ground-based instrumentation. The data gathered by this system is incorporated into a sophisticated data reduction scheme which determines the geodynamic parameters and landmark locations.

Detailed studies were conducted to determine the feasibility of the GOPSS. The study period was designated as Phase I, and the results of these studies have been compiled into five volumes for reader convenience.

This volume describes the effort for implementation of the data acquisition requirements for the GOPSS program. This volume presents the preliminary design which defines and describes the various sensors, considers their functional interdependencies, and shows their evolvement into an integrated GOPSS.

The division of the remaining volumes and their content are now briefly described for information and reference purposes.

Volume 1, Program Compendium and Conclusions, was prepared to provide briefly the details essential to a comprehensive understanding of the effort conducted during Phase I of the GOPSS feasibility study. System concept and objectives are described plus conclusions which concern the attainment or modification of the initial objectives, along with recommendations for a system configuration and a solution of the attendant data handling problems.

Volume 3, Data Reduction, Part 1, considers the photogrammetric data subject to constraints imposed by orbital and auxiliary data, the mapping capabilities of the system, and ground handling of mission photography.

Volume 4, Data Reduction, Part 2, discusses orbital considerations affecting the feasibility of the GOPSS. Physical models and computational procedures are reviewed and error studies involving typical sensor and model inaccuracies are described. Based on these studies, recommendations are made for tracking networks, auxiliary on-board sensors, and detailed orbit plans. In addition, the data reduction procedure whereby the acquired data are simultaneously located to yield geodynamic parameters and landmark locations is considered.

Volume 5, Program Plan, Phases II-V, describes the planning activity as it has been programmed through Phases II to V for the engineering, fabrication, and operational support for the delivery of five systems. Continuing studies which are required are also recommended in this volume.

SUMMARY

A data collection system implements the data gathering phase of the GOPSS program through the use of an orbiting metric camera which photographs all continental land masses and islands, and through auxiliary satellite sensors to provide detail data on satellite position supported by ground based tracking instrumentation.

A preliminary design of the data collection system was completed during the feasibility study. Individual tasks which were accomplished during the study were: (1) the design of a metric lens (fabrication and test are scheduled for completion in February 1967); (2) the preliminary design of a photo-sensor system; (3) a photo-optical analysis to determine the performance of the camera system; (4) an evaluation and selection of auxiliary satellite sensors; and (5) the preliminary design of a recovery section to provide a means of retrieval for photographic data.

The final task was the integration of the sensors into a data collection module, ensuring its design integrity with the recovery section which contains the recovery vehicles, and the interface of both these subsystems to the orbiting control vehicle to accomplish the required system performance.

To establish the required photogrammetric capability, a wide-angle lens has been designed and is being fabricated for the camera system. Lens design progressed through four versions of a 300-millimeter focal length, 80-degree field system. The final selected configuration has three aspheric surfaces, and will yield a 70-line per millimeter AWAR at 1.6:1 contrast on EK type 3404 film.

The resultant photo-sensor system consists of a terrestrial photogrammetric camera and a twin stellar camera which provides a precise attitude reference for the photo-sensor system.

The terrestrial camera consists of the Itek-designed 300-millimeter focal length, f/6.0, wide-angle lens, shutter, IMC drive, platen assembly, film transport assembly, and connecting structure. The twin stellar camera, constructed as a single unit, uses two 250-millimeter focal length, f/1.8 modified Wild Falconar lens assemblies, and is bolted directly to the terrestrial central cell section with the rigidness required to maintain the calibrated knee angles between all three lenses. The stellar lenses are 90 degrees apart, ±45 degrees from the roll axis; they are pointed forward and are elevated 10 degrees with respect to the horizontal.

Lens and camera design factors and environmental factors were analyzed to determine photogrammetric accuracy predictions from all contributing sources. These errors are reflected in an overall system performance estimate. Experimental investigations were also conducted concerning the extension of the AIM curves, film flatness, experimental star recording, and the influence of image quality on measurement accuracy.

The detailed photo-optical analysis of the camera system performance indicates that a minimum resolution of 40 lines per millimeter will be maintained at a 20-degree sun angle on EK 4404 and that 30 lines per millimeter will be maintained at a 5-degree sun angle with EK 3400.

The auxiliary equipment required to implement to the GOPSS operation are configured into the overall payload package. These equipments are the TRANSIT transmitter, radar altimeter, low-g accelerometer, precision clock, and mission data recorder.

Inclusion of the TRANSIT transmitter in the orbiting package allows Doppler tracking by the TRANSIT network. The use of low-g accelerometers aboard the satellite will provide direct information on nongravitational forces acting on the vehicle. The radar altimeter is a complete on-board tracking system which provides an altitude measurement to an accuracy of 10 meters, providing needed information to the photogrammetry and measurement of the geoid fluctuations over the surface of the oceans. The recorder stores time, altitude, and other mission data which will serve as inputs in the data reduction scheme, and has the capability to collect a large quantity of information in small increments. The system clock is a precision oscillator which provides an absolute time reference of less than 1-millisecond error over the entire mission.

The subsystems which comprise the photographic satellite system (see frontispiece) consist of the Orbiting Control Vehicle (OCV), Data Collection Module (DCM), and the Recovery Section (RS).

The OCV provides the required on-orbit propulsion, satellite stability, payload power, and mission control. The OCV sensors provide the signals from which the vehicle is stabilized in roll and yaw, and pitched at a controlled rate. The OCV programmer operates the subsystem equipments through the use of mode signals in any one of four data gathering modes. Two additional photosensor signals, V/h and exposure (t_e), are also supplied from the OCV.

The DCM is connected directly to the front of the OCV and contains the photosensors, radar altimeter, TRANSIT transmitter and clock, and houses the film supply spools. The DCM bay is a cylindrical structure of monocoque design, which is thermally insulated and contains fore and aft fiberglass bulkheads for thermal and light sealing purposes. The payload electronics, radar altimeter, and transponder are packaged as modular units and mounted to the DCM structure. The radar altimeter antenna is mounted below the supply cassettes with its axis pointed down along a yaw axis.

The RS is attached to the forward end of the DCM structure. This section contains the recovery vehicles (RV), each with a recoverable film payload. Two RV configurations were developed, one which has the RV's in line along the roll axis, and the other, the "canted," which has each RV pointed down 60 degrees from the horizontal and aft; the "canted" configuration eliminates the necessity of adjusting the pitch of the vehicle prior to recovery. Each RV contains a recoverable payload consisting of a takeup cassette with spools for 9 ½-inch wide terrestrial film and 70-millimeter stellar film, and a recorder for electronic data storage. A combination cutter and seal is mounted on the bulkhead of each RV to cut the film path and seal the water-tight compartment.

2.1 INTRODUCTION

A data collection system is required to gather inputs for the implementation of the objectives of the GOPSS program. This system consists of both satellite-born sensors and ground tracking instrumentation which supplement each other in orbit determination and in determining the precise location of ground points which will be compiled into a landmark catalog.

Based on the input data determined to be required by the systems analysis of this study, a data collection system was developed which defined the employment of a photosensor, the auxiliary sensors and the ground-based instrumentation that would be necessary and compatible within the prescribed operational environment. Specifics were generated for the individual sensors, functional interdependencies of these sensors were considered, and finally but most important, was the evolvement of the satellite-borne sensors into an integrated payload, properly interfaced with the orbital control vehicle.

Within this integrated concept, Itek developed a payload system responsibility which considered all equipment forward of the orbiting control vehicle as a single assembly. This assembly comprises the section containing the data collection sensors and a recovery section.

Specifically, the data collection module (DCM), contains the photosensor, radar altimeter, TRANSIT transmitter, and a precision clock. The film supply spools are also located in the DCM. The photosensor is composed of a terrestrial photogrammetric camera and twin steller camera configuration. Detailed tasks performed in this area were the design, fabrication, and test of a suitable lens for the terrestrial camera, and a photo-optical analysis to determine the performance of the photosensor system. Lens and camera design factors and environmental factors were analyzed to determine photogrammetric accuracy from all contributing sources.

The recovery section (RS), attached to the forward end of the DCM structure, contains two recovery vehicles (RV). The RV's contain a recoverable film payload which is spooled into a takeup cassette, and a mission data recorder. A combination cutter and seal on the RV cuts the film and seals the RV to ensure a water-tight compartment.

This volume then describes the effort for implementation of the data collection requirements for the GOPSS program.

2.2 DATA COLLECTION SUBSYSTEMS

2.2.1 Photo-Optical Sensor

2.2.1.1 Lens Design, Fabrication, and Test

2.2.1.1.1 Lens Design

1. Design Evaluation

The objective of the lens design task was to design a high resolution, wide angle optical system. Photogrammetric and operational considerations prescribed a lens with a 12-inch focal length and 80-degree field, and a resolution satisfactory to achieve the feasibility program objectives. With this in mind, detail objectives were established and are listed in Table 2-1.

To attain these objectives, the lens design has evolved from the proposal stage to the final GOPSS design through a succession of significant changes and refinements, with associated upgrading of performance predictions. Initial design effort considered a potential modification of the Geocon design by J. G. Baker. This was the only lens in the patent literature that: (1) included a reseau plate, (2) had a field greater than 80 degrees, (3) was faster than f/6.0, (4) was shorter than three focal lengths, and (5) had a potential of meeting a minimum low contrast resolution of 25 lines per millimeter. It was setup as described in the patent literature; it was scaled to a focal length of 12.0 inches, the aperture was reduced from f/3.5 to f/6.0, and the field decreased from 94 to 80 degrees. The geometrical transfer functions were solved in three colors from 0.54 to 0.70 micron. The computed AWAR of the lens was approximately 33 lines per millimeter, and the minimum resolution, at the worst orientation point, was 7 lines per millimeter at 1.6:1 contrast on Eastman Kodak (EK) type 3404 film. This lens was designed for negligible distortion and a flat field. Relaxing these requirements as well as optimizing for the lens f/number, field, spectral range, and film choice resulted in an increase in AWAR from 33 to 75 lines per millimeter at the expense of a 0.2-inch deformed image and 0.2-inch distortion. The minimum resolution remained at 7 lines per millimeter because of an oversight concerning the control of rays outside the sagittal and tangential fans. The new lens had the original high index glasses in the optical elements which are not available in the size necessary for a 12-inch focal length objective.

The first configuration studies made after the contract was awarded utilized negative elements on the outside, as exemplified by Bertele's Aviogon, Roosinov's patent, and Gray's work during World War II. A reseau plate, aspherics adjacent to the stop, and an aspheric image were utilized. The starting point was an 11-element Bertele design with a flat field, no aspherics, and minimum monochromatic resolution of 7 lines per millimeter. This design had low index glass for the outer elements and approximately $\cos^3 \theta$ illumination drop-off. The Preliminary I (P-I) design indicated that with BK-7 used in the outer elements, minimum resolutions exceeding 25 lines per millimeter would be obtained; for this reason, the Geocon approach was abandoned.

Table 2-1 — Comparison of Proposed and Final GOPSS Lens Design

			Objective	Final GOPSS Design
1.	Focal length		300 millimeters	300 millimeters
2.	f-ratio		f/6.0	f/6.0
3.	Format		230 by 460 millimeters	230 by 460 millimeters
4.	Total field angle		80 degrees	80 degrees
5.	Spectral region		0.54 to 0.70 micron	0.60 to 0.70 micron
6.	Film		EK 3404	EK 3400
7.	Glass reseau plate		Provided	Provided
8.	Reseau back and film surface		Aspheric	Flat
9.	Maximum distortion		0.10 inch	0.055 inch
10.	Minimum relative illumination		40 percent	40 percent
11.	Elements (without reseau)		10 to 12	10
12.	Aspheric surfaces		3	3
13.	Low contrast (1.6:1) resolution, lines per millimeter			
	a. On-axis	3404		125
		3404		64
	b. Minimum over entire format	3404	25 lines per millimeter	40
		3400		30
	c. AWAR	3404		≈ 70
		3400		≈ 48
14.	High contrast resolution, lines per millimeter			
	a. On-axis	3404		180
		3400		112
	b. Minimum over entire format	3404		greater than 50
		3400		greater than 50
	c. AWAR	3404		≈100
		3400		≈ 70

The completed Preliminary II (P-II) design had a minimum resolution in all orientations, and fields of 30 lines per millimeter on a 0.012-inch sag from aspheric image surface, which was significantly flatter than the proposed value of 0.12 inch. The distortion, as measured on a flat field, was approximately 0.12 percent. Optical glass was ordered for lens fabrication specifying oversize blanks for the elements in this design.

The reduction in aspheric field sag from 0.5 inch in the proposal to 0.012 inch for the P-II design, raised the minimum resolution from 7 to 30 lines per millimeter and indicated that a 25-line per millimeter minimum on a flat field might be attainable.

The aspheric surface on the reseau plate was placed on the side opposite the film, permitting a flat field. This configuration (P-III) resulted in the first flat field design having a minimum resolution that exceeded 25 lines per millimeter (Modulation = 0.12) on EK type 3404 film at 1.6:1 contrast with a 0.54- to 0.70-micron spectral range.

To reduce the metric errors caused by the secondary lateral color blur which is proportional to the square of the spectral bandwidth, the region was reduced from the old value of 0.54 to 0.70 micron to 0.60 to 0.70 micron. This reduction in spectral bandwidth also improved the lens modulation transfer function at frequencies of 20- to 30-line per millimeter resolution.

2. Final GOPSS Lens Design

The final GOPSS Design utilizes the 0.60- to 0.70-micron spectral region and EK type 3400 film (refer to Figure 2-1). The specifications for the final lens design are given in Table 2-2. The minimum resolution on EK type 3404 film is 40 lines per millimeter on a flat field compared to the proposal estimate of 25 lines per millimeter on EK type 3404 film using a 0.1-inch deformed image surface; on-axis performance is 125 lines per millimeter with an AWAR of 70 lines per millimeter. Table 2-1 lists the performance of the final design in comparison with the initial goals. Ray-trace results and geometric transfer functions (Figures 2-2 through 2-4) show reduced higher order aberrations and chromatic blur, as well as the increased contrast in the transfer function.

3. Optical System Studies

a. Image Position Displacements Caused by Mechanical Changes

Calculations were made to determine the sensitivity of the camera calibration to small displacements of the optical components. Changes in tip, decentering, and spacing were studied (see Table 2-3). Three cases were taken as being representative: (1) the movement of the front element within its cell, (2) the movement of the front half of the lens with respect to the rest of the camera, and (3) the movement of the entire lens with respect to the platen. The front element is considered to be the most sensitive single element because of its power, size, and distance from the stop. Since the two halves of the lens cell and the platen are different structural units, the possibility of their moving relative to each other was considered.

Calculations were made, using computer ray traces where necessary, to determine the effects of 0.0001-inch decentering, 5×10^{-6} radian tip (0.0001-inch at a radius of 20 inches), and 0.0001-inch spacing change. The maximum radial image shifts are plotted as functions of image position for the three separate cases shown in Figures 2-5, 2-6, and 2-7.

Table 2-2 — Final Lens Design Specification Sheet (9240 Wide Angle System, Melt 1A)

Element Number	Surface Number	Radius, inches	Radius Tolerance, ± inches	Thickness, inches	Thickness Tolerance, inches	Airspace, inches	Airspace Tolerance, inches	Clear Aperture, inches	n*	v†	Glass Type and Melt
I	1	27.7896	0.0072	0.8000	0.0050			12.769	1.51514	64.02	BK-7 14097
	2	6.5414	0.0010			1.6500	0.0040§	9.976	Air		
II	3	12.0615	0.0021	0.9437	0.0050			9.715	1.51416	64.07	BK-7 14176
	4	9.5482	0.0014			2.1725	0.0030§	8.918	Air		
III	5	7.5519	0.0013	3.0022	0.0030			7.580	1.71673	50.35	LAK-10 80980/1
	6	2.5844	0.0006	0.0004				4.659	1.55063		Cement M62
IV	7	2.5844	0.0006	2.3692	0.0020			4.659	1.61508	49.72	SSK-8 310543/44
	8	-4.9491	0.0017	0.0004				4.377	1.55063		Cement M62
V	9	-4.9491	0.0017	0.9493	0.0020			4.377	1.60281	40.28	BaSF-3 13893
	10*	29.3694				0.7742	to be adjusted	3.272	Air		
	11	"		Aperture stop		0.5602		2.388	Air		Aperture stop
VI	12*	18.6093		0.5016	0.0040			3.325	1.55083	51.22	BaLF-8 13906
	13	5.5566	0.0030	0.0004				3.884	1.55063		Cement M62
VII	14	5.5566	0.0030	2.1803	0.0040			3.885	1.61079	51.24	SSK-3 330763/1
	15	-2.9840	0.0010	0.0004				4.435	1.55063		Cement M62
VIII	16	-2.9840	0.0010	0.5000	0.0020			4.435	1.71136	29.48	SF-1 340756/29, 32
	17	-6.2808	0.0020			5.8752	0.0020§	5.120	Air		
IX	18	-4.9664	0.0008	0.6713	0.0040			7.876	1.51416	64.07	BK-7 14176
	19	-10.5045	0.0016			1.9500	0.0030§	9.562	Air		Air
X	20	-6.3356	0.0010	0.7326	0.0040			10.202	1.51514	64.02	BK-7 14097
	21	-11.8946	0.0011			1.9255		12.640	Air		Air
XI	22‡	226.1301		0.7099	0.0050			19.158	1.51483	64.06	BK-7 14102
	23	"				0.0001		20.145	Air		Air
	24	"		Image plane				20.144			

* Refractive index at 6500 angstroms

† Reciprocal dispersive power at 5876 angstroms

‡ Aspheric with coefficients as follows:

	Fourth Order	Sixth Order	Eighth Order	
Surface 10	$+2.566 \times 10^{-4}$	-7.086×10^{-5}	-1.160×10^{-5}	-7.537×10^{-7}
Surface 12	$+4.960 \times 10^{-4}$	$+1.113 \times 10^{-5}$	-2.120×10^{-6}	$+3.547 \times 10^{-7}$
Surface 22	-1.111×10^{-4}	$+5.640 \times 10^{-7}$	$+8.031 \times 10^{-10}$	0.0

§ The airspace thicknesses given will be subject to change in a redesign after the test spheres are made and measured. Elements I, II, IX, X, XI may be completely fabricated at this time using the above data. The inside triplet elements are subject to changes in central thicknesses; therefore, only one surface per element may be completely fabricated at this time.

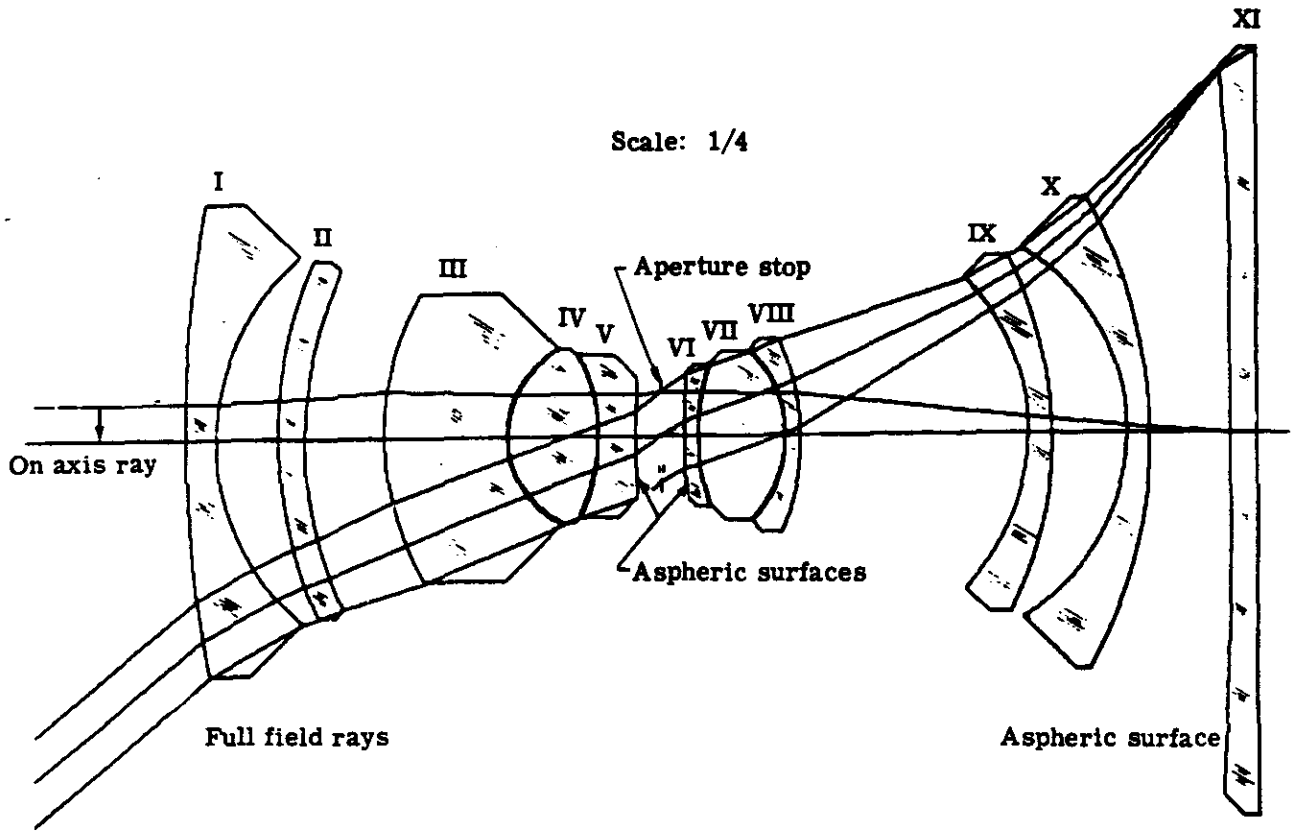

Element	I	II	III	IV	V	VI	VII	VIII	IX	X	XI
Glass Type	BK7	BK7	LAK10	SSK8	BaSF3	BaLF8	SSK3	SF1	BK7	BK7	BK7

Fig. 2-1 — GOPSS lens design

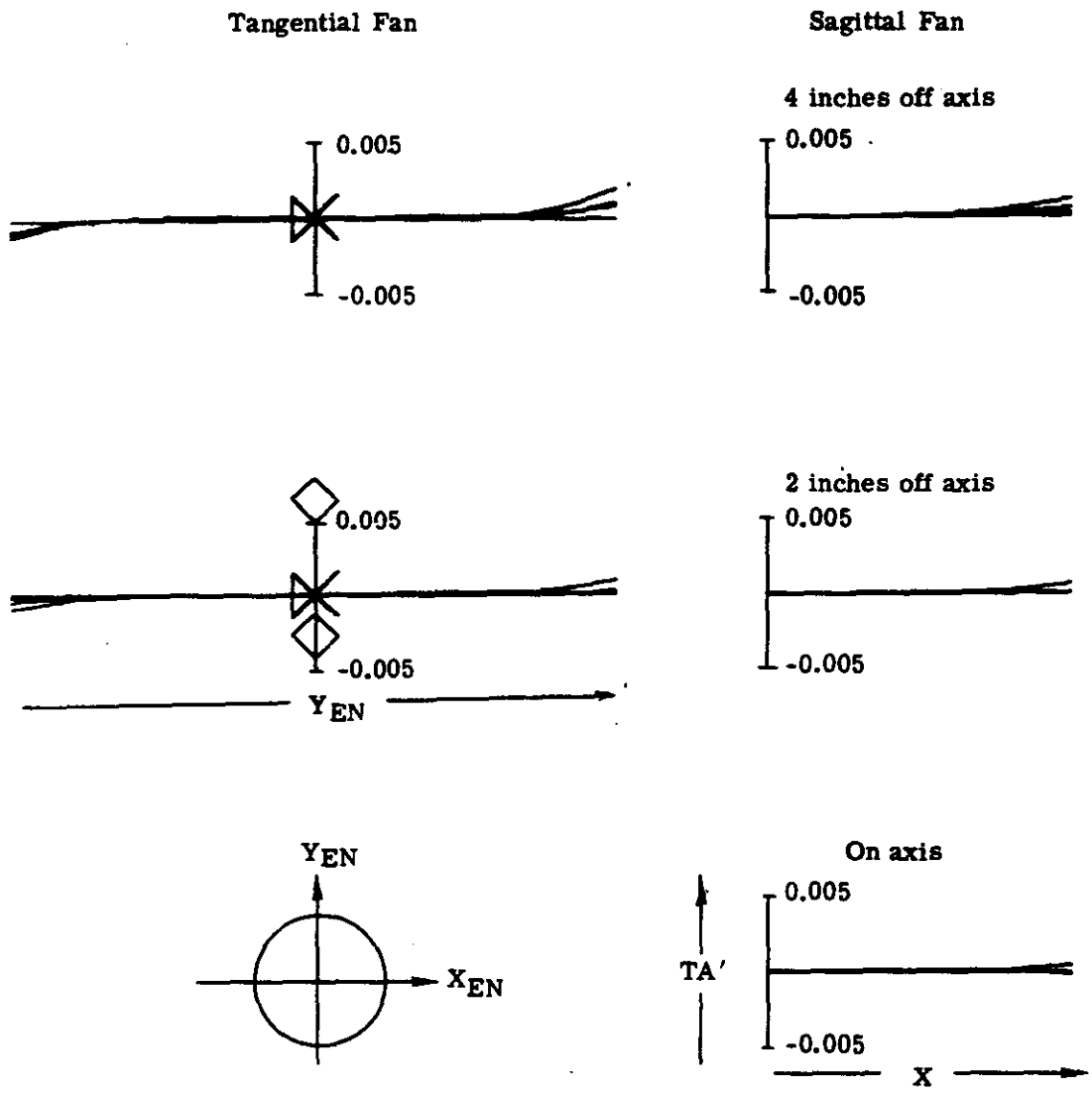

NOTE: TA' = transverse aberration

Fig. 2-2(a) — Ray trace plots for GOPSS lens design (on-axis to 4 inches off-axis)

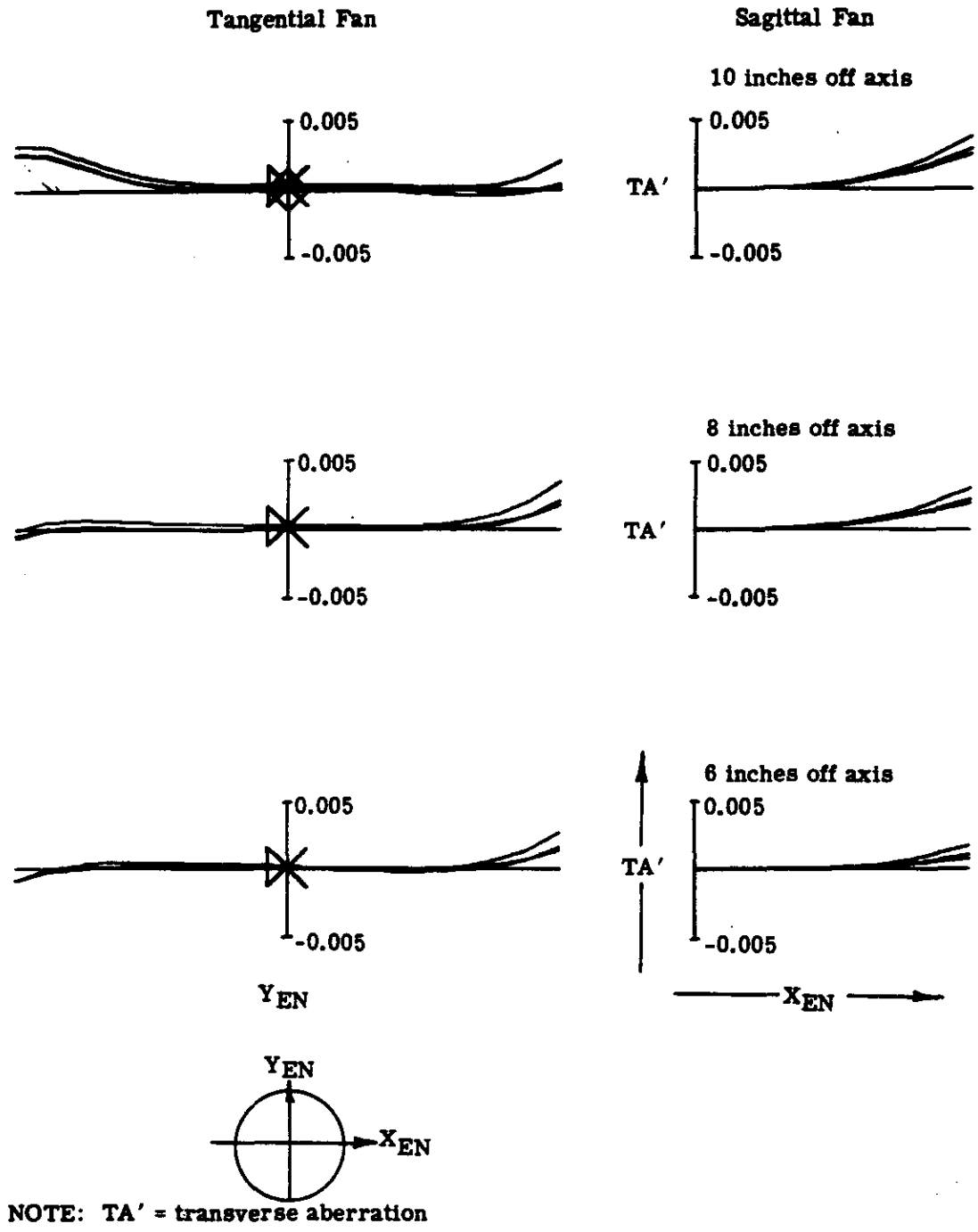

NOTE: TA' = transverse aberration

Fig. 2-2(b) — Ray trace plots for GOPSS lens design (6 inches to 10 inches off-axis)

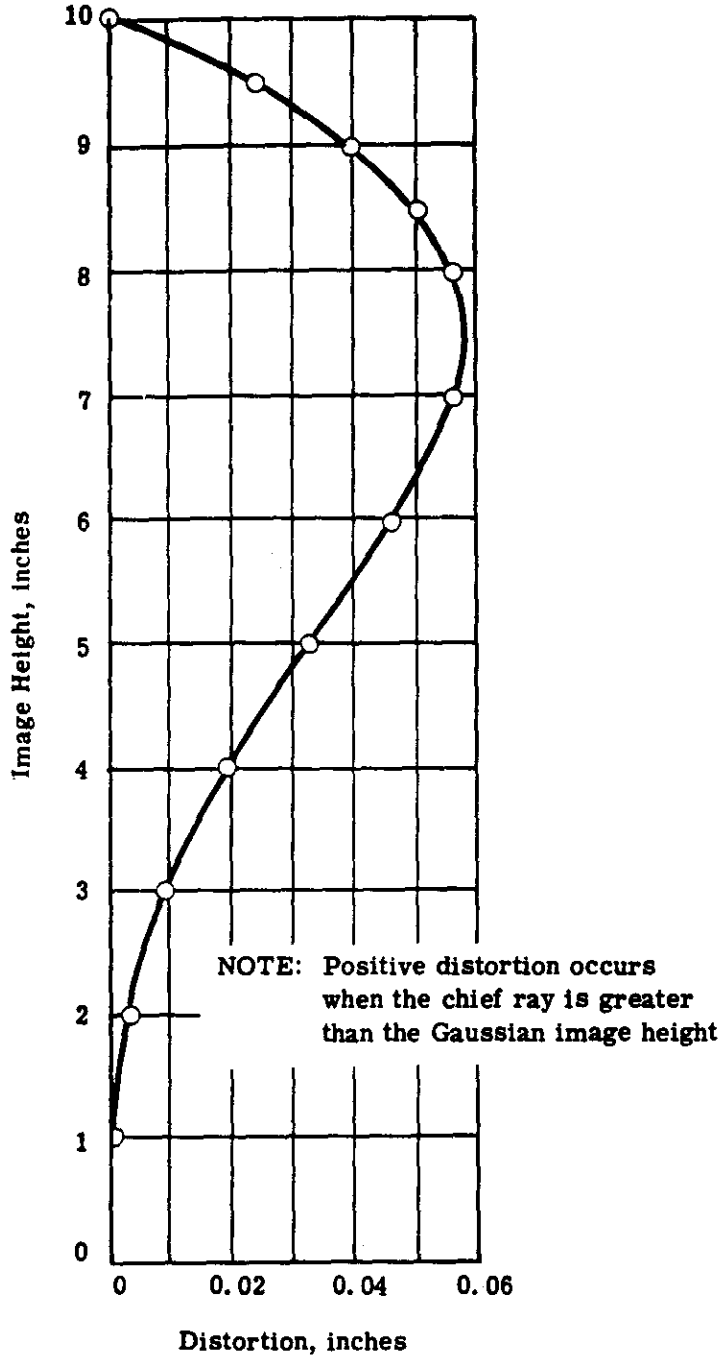

Fig. 2-3 — Distortion plot

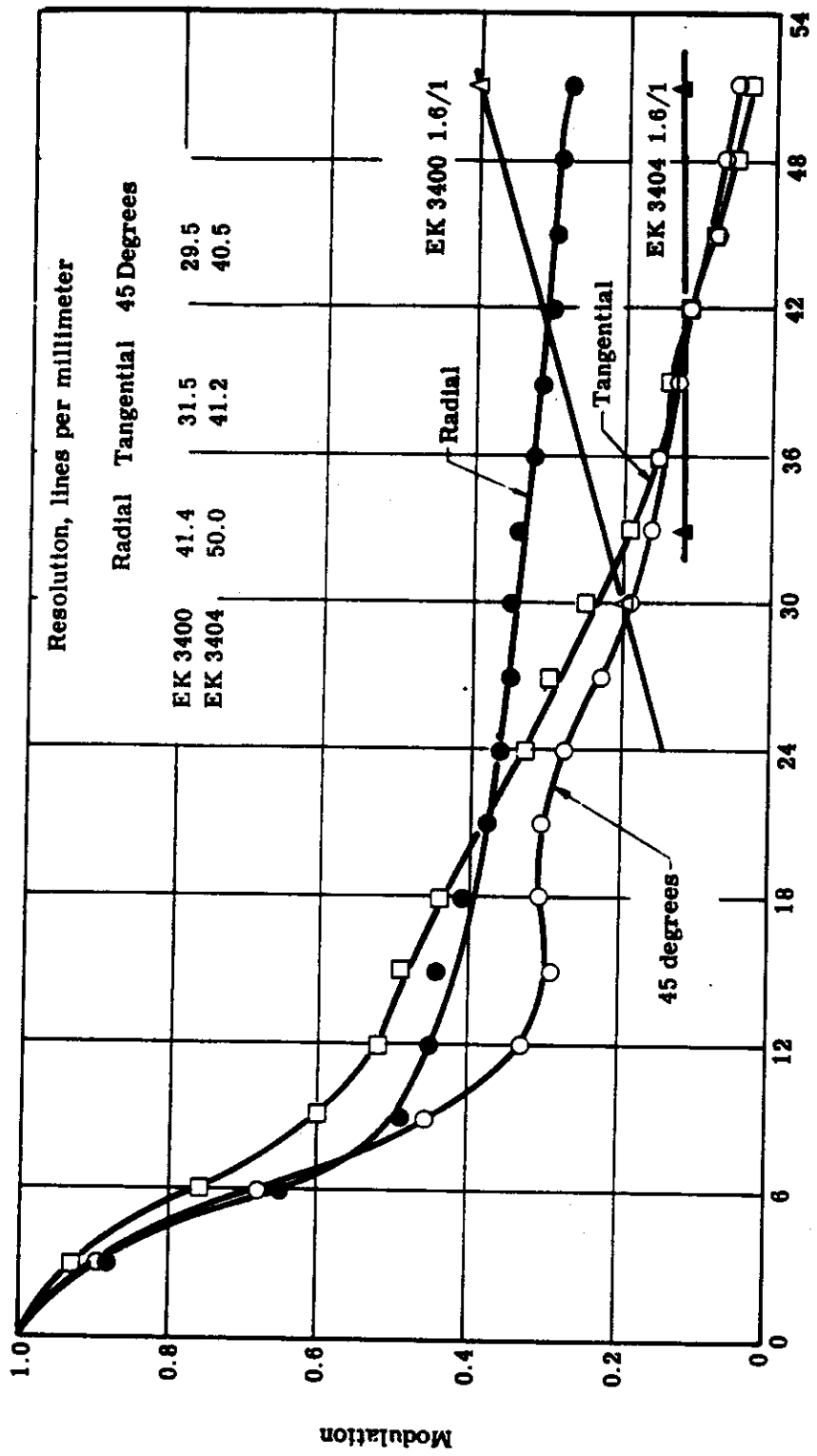

Fig. 2-4(a) — Geometrical frequency response: semifield height = 10.0 inches, deflection = +0.002 inch, spectral region = 0.60 to 0.70 micron

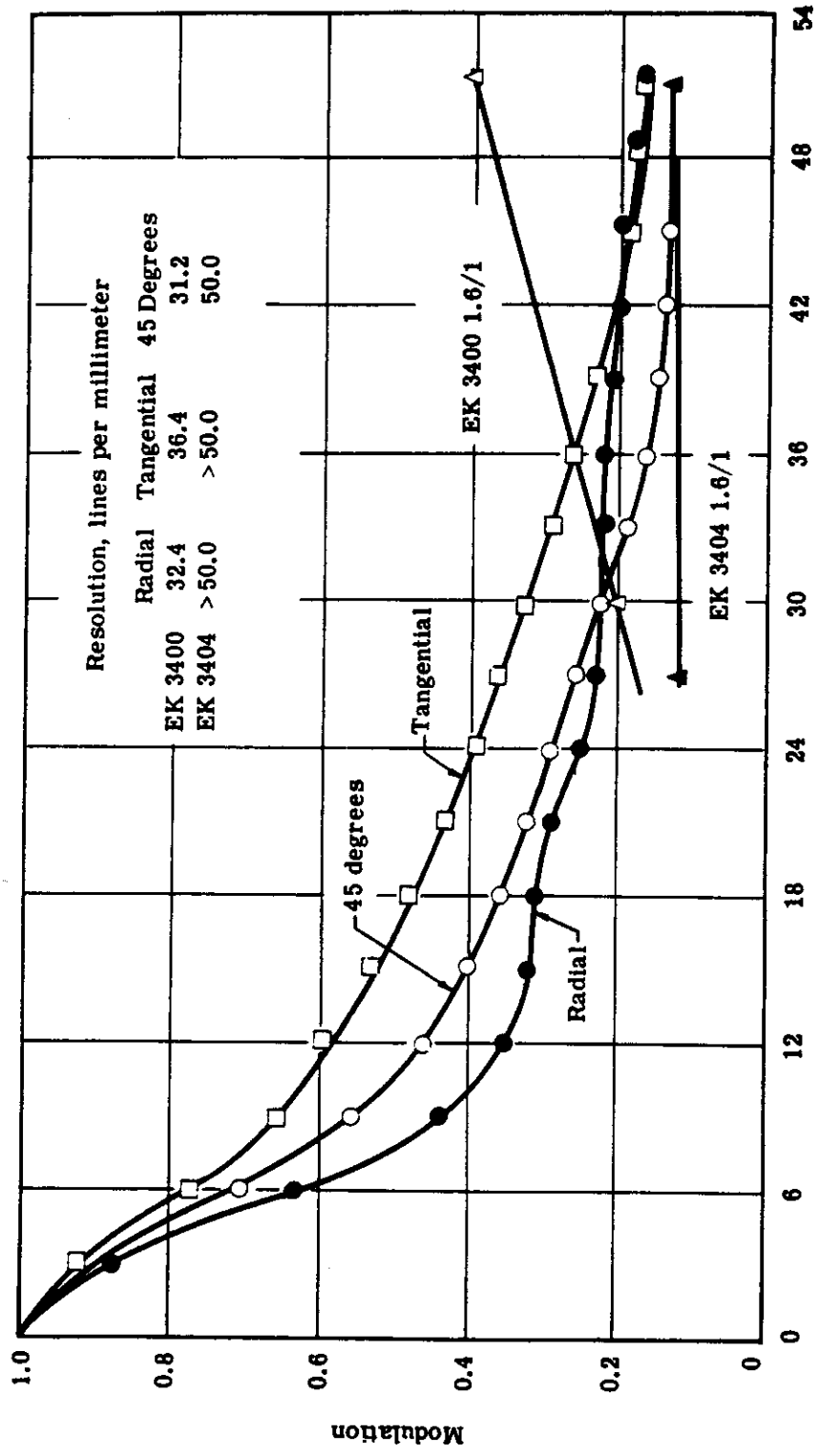

Fig. 2-4(b) — Geometrical frequency response: semifield height = 8.5 inches, deflection = +0.002 inch, spectral region = 0.60 to 0.70 micron

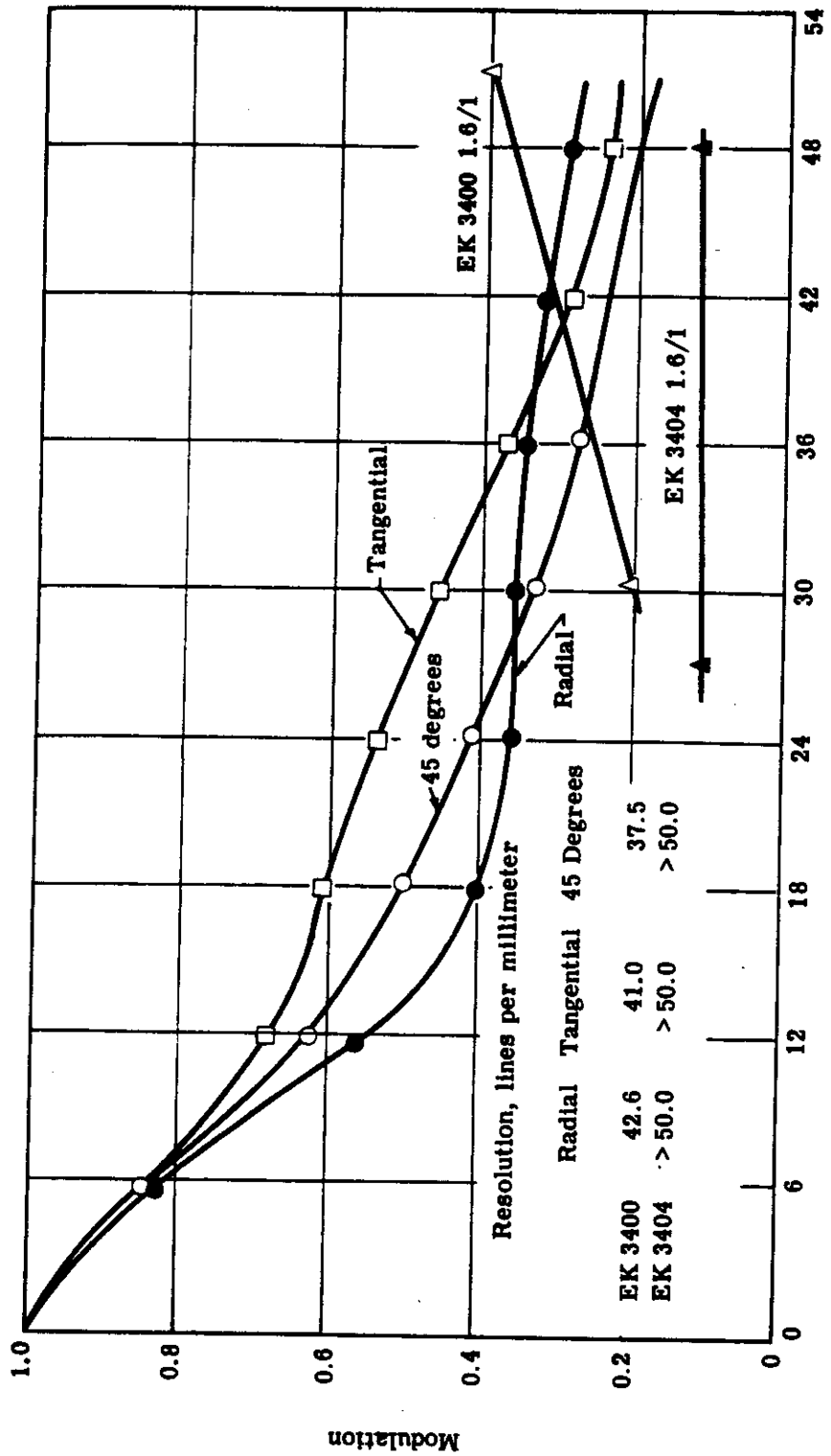

Fig. 2-4(c) — Geometrical frequency response: semifield height = 7.0 inches, deflection = +0.002 inch, spectral region = 0.60 to 0.70 micron

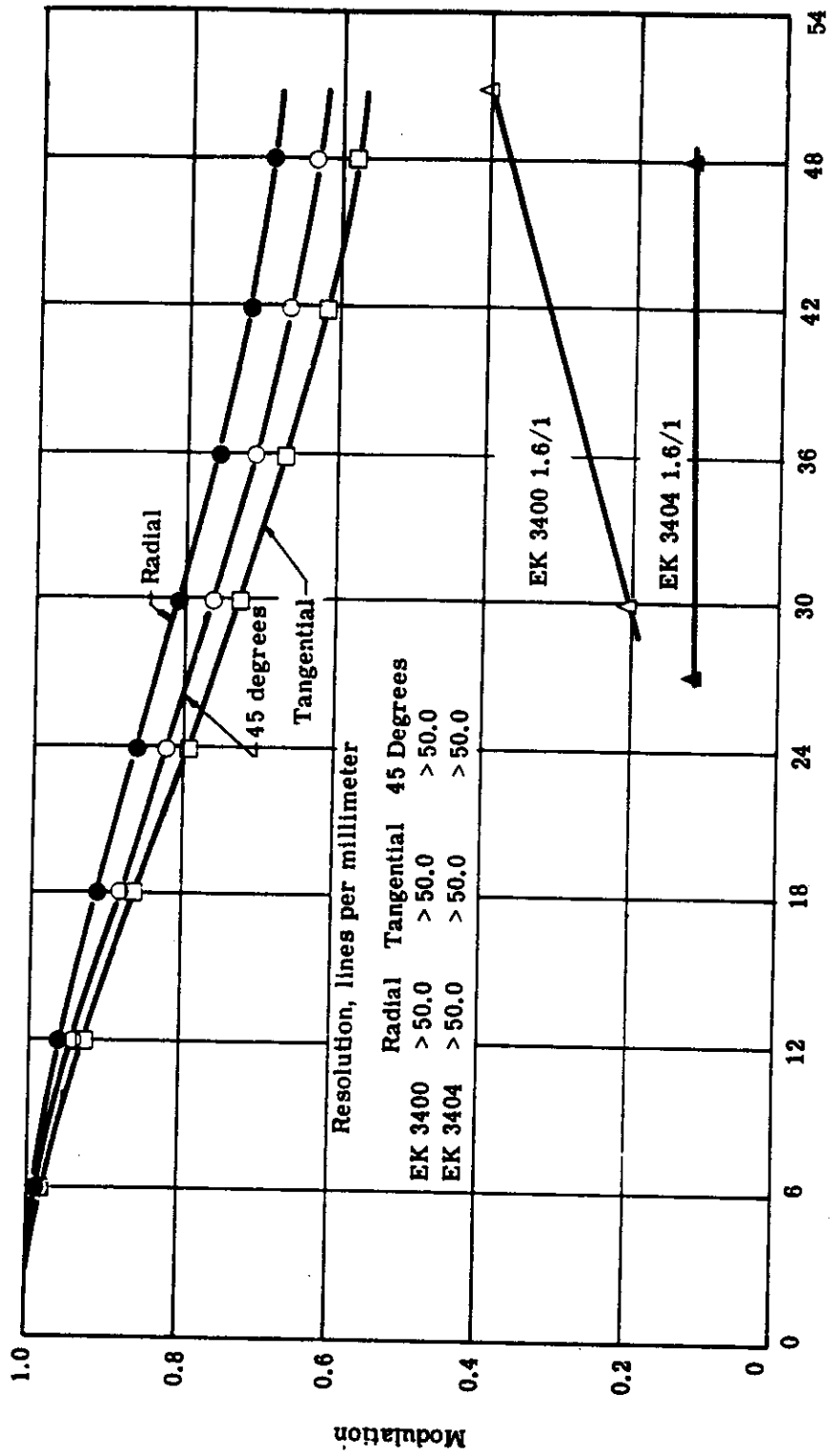

Fig. 2-4(d) — Geometrical frequency response: semifield height = 3.5 inches, deflection = +0.002 inch, spectral region = 0.60 to 0.70 micron

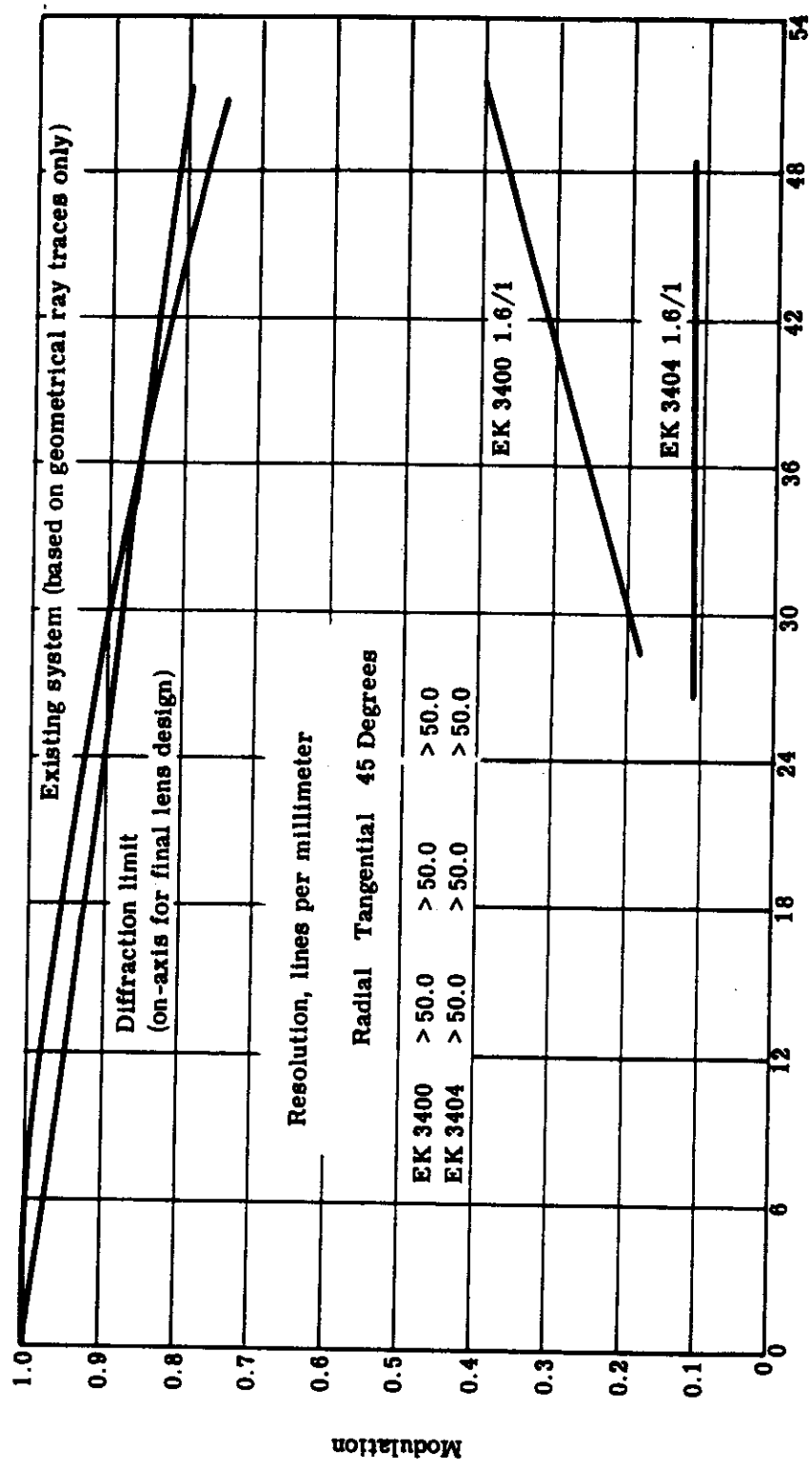

Fig. 2-4(e) — Geometrical frequency response: semifield height = 0.0 inch, deflection = +0.002 inch, spectral region = 0.60 to 0.70 micron

Table 2-3 — Effects of Tilt, Decenter, and Spacing Error

	Nominal System		Element I		First Half of System		Element I	First Half of System
			Decenter, 0.001 inch	Tilt, 0.00005 radian	Decenter, 0.001 inch	Tilt, 0.00005 radian	ΔAir Space, 0.001 inch	ΔAir Space, 0.001 inch
$\bar{H}$	Distortion	Chief Ray Height	Chief Ray Height	Chief Ray Height	Chief Ray Height	Chief Ray Height	Chief Ray Height	Chief Ray Height
0.0	0.0	0.0	-0.0007132	-0.0003712	-0.0002435	-0.0007169	0.0	0.0
0.2	0.0027414	2.0165335	2.0157966	2.0161511	2.0162714	2.0157965	2.0163566	2.0164847
0.4	0.0187631	4.0463473	4.0455404	4.0459312	4.0460293	4.0455503	4.0459772	4.0462326
0.6	0.0455573	6.0869336	6.0860195	6.0864673	6.0865210	6.0860490	6.0863379	6.0867207
0.7	0.0551399	7.1034122	7.1024353	7.1029167	7.1029382	7.1024794	7.1026889	7.1031347
0.8	0.0549699	8.1101383	8.1090947	8.1096122	8.1095946	8.1091533	8.1092840	8.1097807
0.9	0.0385507	9.1006151	9.0995026	9.1000580	9.0999947	9.0995801	9.0996315	9.1001666
1.0	-0.0000327	10.0689276	10.0677461	10.0683393	10.0682246	10.0678448	10.0678439	10.0683769

Maximum Radius Deviation of 30 Percent Spot Size (tolerance is 0.00003 inch)

	Decenter, 0.001 inch	Tilt, 0.00005 radian	ΔAir Space, 0.001 inch	Deflection for ΔAir Space
Element I	-0.00011108	-0.00008469	-0.00004248	-0.0010370
First half of system	-0.00030872	-0.00006206	-0.00018690	-0.0002765

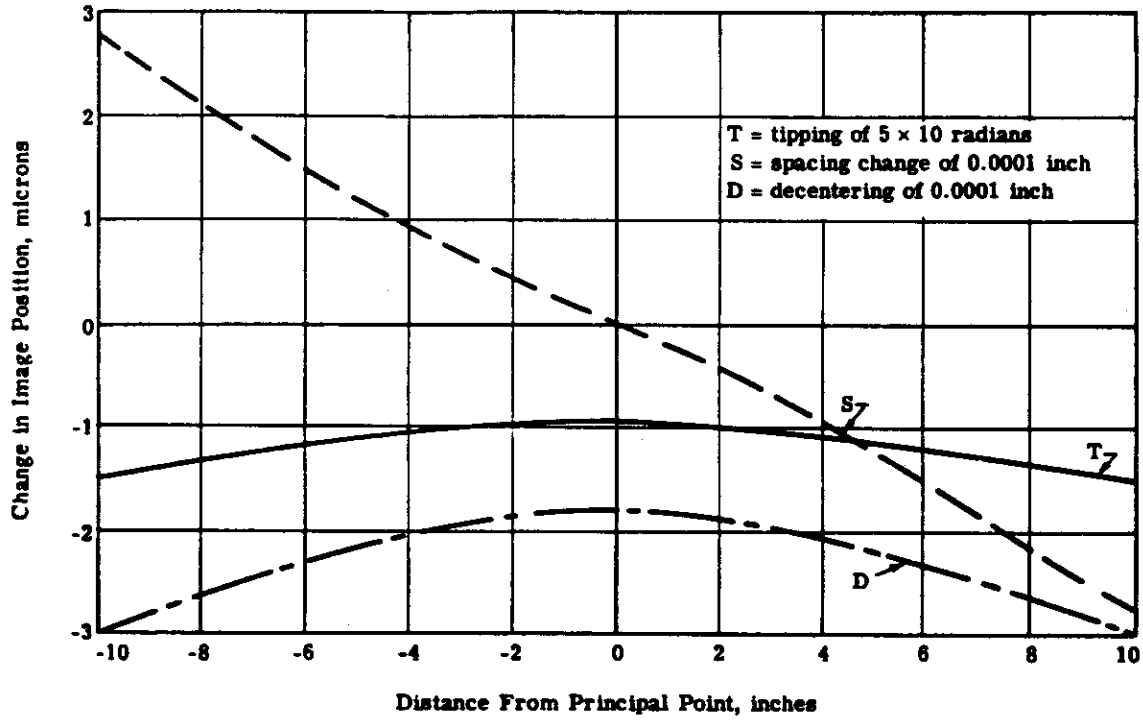

Fig. 2-5 — Effects of change in position of the front element

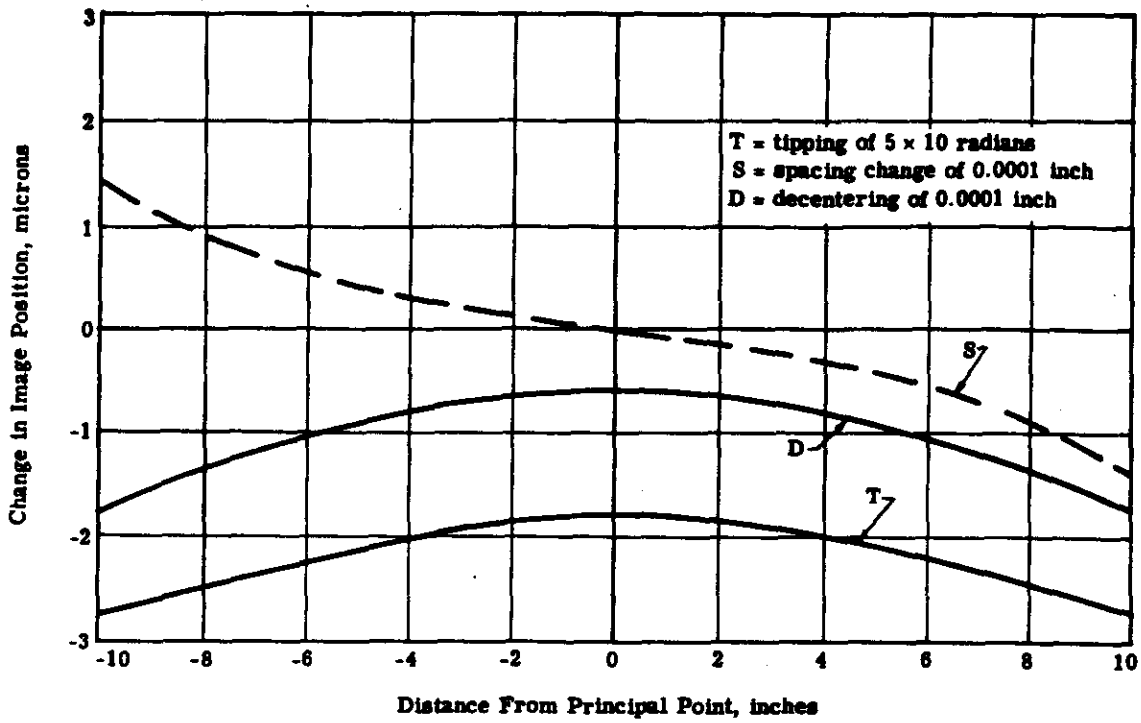

Fig. 2-6 — Effects of change in position of the front half of the lens

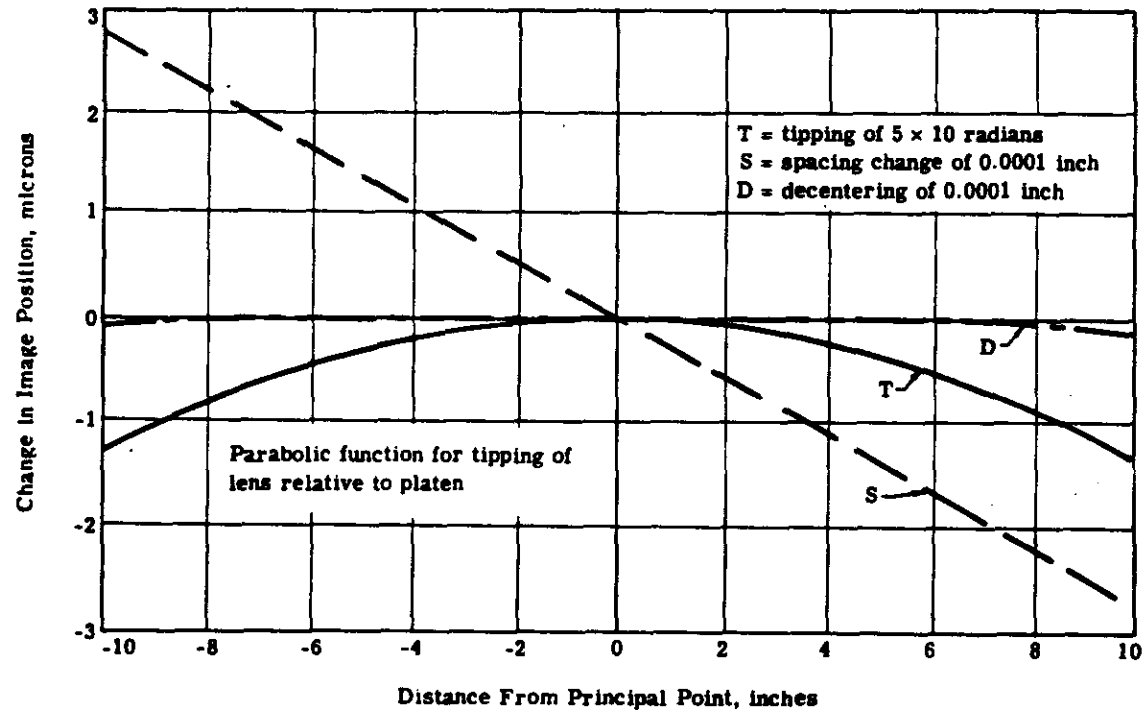

Fig. 2-7 — Effects of change in position of lens relative to the platen

Examination of these curves indicates the degree to which changes in the lens distortion pattern after calibration can be corrected by on-orbit recalibration. The errors produced by spacing changes can be partially removed by focal length recalibration done from on-orbit star photographs. In the case of movement of the front element alone, shown in Figure 2-5, the image displacements are almost exactly proportional to the image heights. This indicates a simple magnification change and is removed almost completely by focal length recalibrating. In this case, the residual error, or uncompensated change in the distortion, is less than 0.1 micron. In the case of a change of the central air spacing (refer to Figure 2-6), the residual error after focal length recalibration would be about 0.3 micron. Axial movement of the platen produces very nearly pure scale change (refer to Figure 2-7). Again, the residual error after focal length recalibration is less than 0.1 micron.

Tip and decentering cannot be compensated by scale recalibration since, as shown by the curves, the image is shrinking in one half of the format but expanding in the other half. This effect is similar to the effects of tipping the camera slightly away from vertical, with the resulting increase in scale factor in one half the picture and decrease in the other half. In fact, tip of the platen has exactly the effect of tilting the camera out of vertical. In each case, the image movement is a parabolic function of image height in the format. By comparison with the platen tip curve, the tip and decentering functions of the front element and the front half of the lens are also seen to be very close to the parabolic form of the function for tilting of the camera. This apparent tilt of the camera should become evident from the photogrammetry or, for that matter, from the on-orbit stellar photographs used for the focal length recalibration; it can be corrected, except for residuals on the order of 0.1 micron, the amount by which the tip and decentering curves deviate from a true parabola.

The tip and decentering curves for the front element and the front half of the lens show, as well as a parabolic form, a constant displacement from the origin. This movement of the image at the center of the format is a shift of the principle point, and gives, when multiplied by the focal length, an apparent change in the pointing angle of the camera relative to the rest of the system. This change can be compensated, therefore, by recalibration of the knee angle with the on-orbit stellar photographs.

In conclusion, it is seen that the camera can suffer surprisingly large changes in its structural dimensions without any serious impairment of its photogrammetric capabilities. While changes in the positions of the elements on the order of 0.0001 inch, and tips on the order of 5×10^{-6} micron, are intolerable if uncalibrated, it appears (for the cases examined) that all but a few tenths of a micron distortion can be compensated, because changes in the image caused by movements of the individual elements all fall into the same basic pattern. Complete distortion recalibration is therefore unnecessary; measurements of image position movements at a relatively few points are sufficient, and several on-orbit star photographs should be sufficient to make the corrections.

b. Lens Cell Materials

Studies have been made to determine the material with the optimum thermal characteristics for the lens cell. Three materials with a widely different coefficient of expansion were considered for the lens cell/camera construction. Cameras of all invar, all beryllium, and all aluminum construction were analyzed. The metric fidelity of the camera was found for (1) a uniform change in temperature of the whole camera system, (2) a change in temperature of the front half of the lens, and (3) a change in temperature of the front element only.

Of the three materials studied, only beryllium appeared to provide a real advantage for the present system. The change of image size with temperature level for an all beryllium camera construction is closely matched by the change in size of the reseau plate. For this type of change the camera can be expected to keep its calibration regardless of operating temperature. Figure 2-8 shows the plots for beryllium construction.

When the front half of the system was raised 10 °F above the rest of the camera, an image point at the corner of the format moved about 7 microns toward the center. When the front element alone was raised in temperature by 10 degrees, the image at the corner moved toward the axis by about 6 microns. Invar construction for the system reduced the error in the former case from 7 to 5 microns, but had no effect on the change caused by temperature difference of the front element.

While it is theoretically possible to provide a system which is insensitive to these temperature differences, as well as being insensitive to overall temperature level, the construction would require materials of several different coefficients of expansion. In this construction it appears likely that the fit of the lens elements in their cells would suffer. The mechanical errors would then become far more serious than the thermal errors. On this basis, the better procedure appears to be the controlling of the temperature difference throughout the system. This is the approach presently planned.

c. Shift of Focus Corrections

The camera will be fabricated, assembled and tested under normal atmospheric temperature and pressure. The final focusing, however, must be correct for the operational environment in which the system will operate. The focus changes to be expected between atmospheric pressure and vacuum have been calculated. In addition, the temperature shift of focus under vacuum conditions has been determined. These values are as follows:

Condition	Shift of Focus, inches
Change of pressure of 1 atmosphere	-0.017
Camera system temperature of +10 °F	+0.001
Front half of system raised +10 °F	+0.001
Front element raised +10 °F	+0.0001

With the exception of the pressure shift, the focal shifts appear to be insignificant in terms of their effect on image quality.

d. Thermal Gradients in the Front Element

Because this design requires front elements which are considerably larger in diameter than the entrance pupil, the image forming rays for different field points will pass through different sections of the front element. Therefore, a change at one edge of the front element can shift the image points at one edge of the format without changing the position of image points over the rest of the format. This shift appears as a measurement error.

If this error is radially symmetrical and constant, it may be partially removed through stellar recalibration of the scaling factor, or calibrated equivalent focal length. Since it is probable that the gradient will not be constant and possibly not completely symmetrical, a limit as to the permissible gradient has been determined.

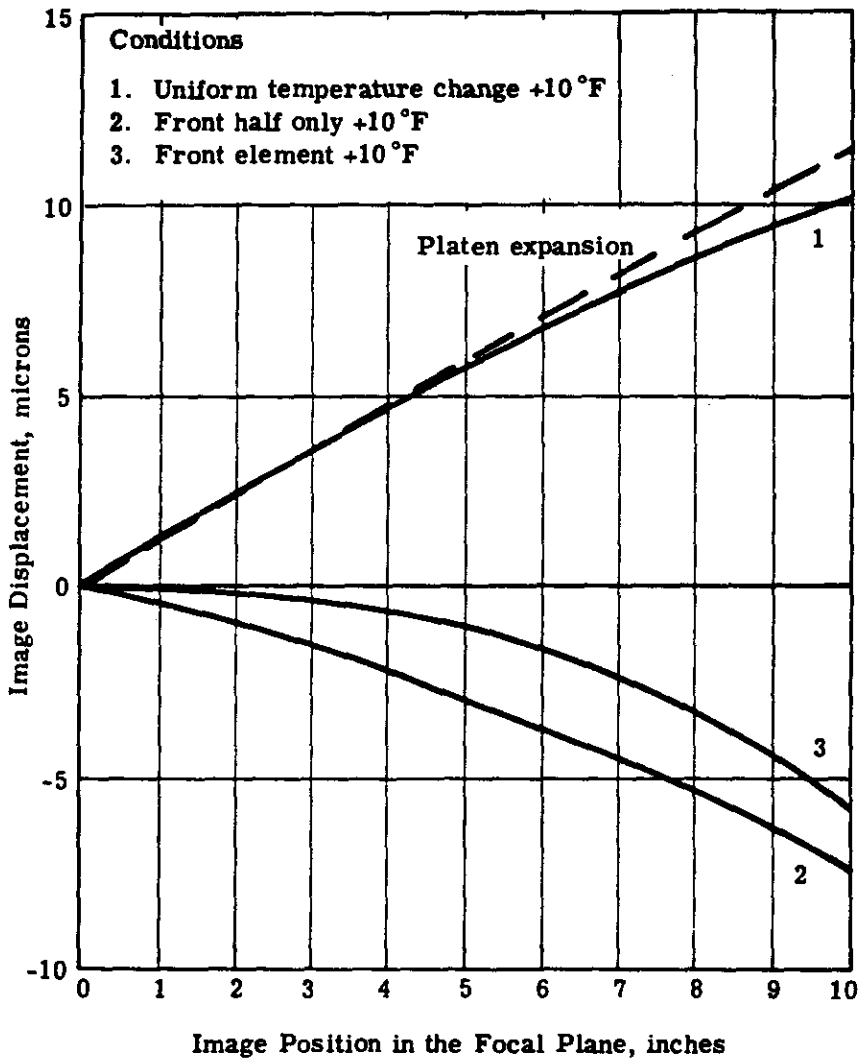

Fig. 2-8 — Thermal behavior of terrestrial camera in vacuum (cell material-beryllium)

The gradient, by differential thermal expansion of the glass, generates a slight wedge; in addition, by the change of index of refraction with temperature it produces a gradient of index in the piece which also deviates the light rays. These effects are additive. Generally, the effect of the thermal expansion is the major source of trouble, being several times as large as the effect of the index gradient.

The calculation for the effect of a 1 °F per inch gradient in a block of glass is shown below.

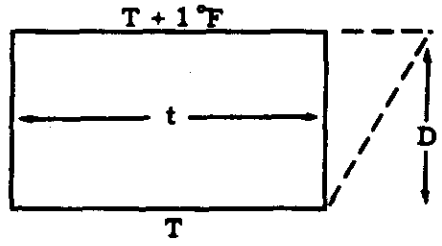

The expansion of BK-7 glass per degree Fahrenheit is $\alpha = 4.6 \times 10^{-6}/°F$. The deviation caused by this expansion is

$$\delta_1 = \frac{t}{D} \alpha (n - 1) = \frac{t}{D}[4.6 \times 10^{-6} (0.516)]$$

The effect of change of index with temperature $0.84 \times 10^{-6}/°F$ is to retard the wavefront at one side by an amount equal to $t\Delta n$.

The deviation caused by this retardation is directly

$$\delta_2 = \frac{t}{D} \Delta n = \frac{t}{D} (0.84 \times 10^{-6})$$

Or the total deviation is equal to

$$\delta = \delta_1 + \delta_2 = \frac{t}{D}[4.6 \times 10^{-6} \times (0.516) + 0.84 \times 10^{-6}]$$

$$\delta = \frac{t}{D} (3.2 \times 10^{-6})$$

The thickness of glass for the front element for the principal ray at the 40-degree field angle is 2.2 inches. The deviation of this ray produced by a lateral 1 °F per inch temperature gradient is then

$$\delta = \frac{2.2}{1.0} (3.2 \times 10^{-6}) = 7.0 \times 10^{-6} \text{ radian}$$

The displacement in the focal plane caused by this deviation is

$$s = \delta f / \cos^2 40$$

$$s = 7.0 \times 10^{-6} \times 305 \times 10^{3} \times 1/0.586 \text{ (microns)}$$

$$s = 3.6 \text{ microns}$$

Results indicate a thermal gradient of one Fahrenheit degree per inch will cause a maximum image point shift of 3.6 microns.

2.2.1.1.2 Lens Fabrication and Test

1. Tolerances

A thorough investigation into optical alignment and fabrication procedures required to achieve a complete system commensurate with the optical design effort has been conducted jointly by the Itek optical design department, the optical shop engineers, and the system engineers. Image sensitivity to element tilts, decenters, central thicknesses, air space thicknesses, and surface radii require the tolerancing of some 60 odd parameters. The feasibility of maintaining these tolerance requirements has been examined .

The radius, decenter (or wedge), and tilt tolerances can be maintained through normal shop procedures. However, the central thickness tolerances of the elements are extremely tight and require a modification of normal procedures, but can be met. A special center-thickness measuring fixture has been designed and built to ensure sufficiently accurate control of the element center thickness (see Figure 2-9). The generation of exact tolerance values for all the above mentioned parameters has been completed for the final optical design.

Image quality sensitivity to misalignment errors and to central thickness errors for the final design has been studied. Image quality for static environment is based upon a 30 percent allowable increase in image spot size throughout the field. Image quality for the dynamic case (fixed image plane) is based largely upon the effect on variation of distortion. The tolerancing has been concentrated on the elements in the two cemented triplets since image quality is more sensitive to their alignment. The procedure given in the following paragraph minimizes these errors. The bar graphs in Figure 2-10 illustrate the combined effect to image quality due to alignment errors and to inherent mechanical errors in fabricating these elements.

During the cementing process, the triplet elements will be positioned utilizing either an air or electronic gauge to read total indicated run-out normal to the exposed surface of the rotating element as shown in Figure 2-11. In addition to an approximately 30-microinch decentering error in either gauge, there is also a mechanical error inherent in the present edging table resulting in a possible 25-microinch decentering error in each element. These error values are used through analytical equations to determine the maximum possible error which may exist in the triplets after cementing. Each element is then decentered and/or tilted by these calculated values and then ray-traced to determine the effect on image quality.

The major aberration due to a change in central thickness of an element is astigmatism, which increases as the square of the field angle. The wide field angle of this system thus increases the requirement in the fabrication of central thicknesses within allowable tolerances. However, the number of elements requiring this extreme accuracy in measuring may be greatly minimized or even eliminated by the following procedure. After each element is completed, its central thickness is measurable to 5×10^{-6} inch which is within the required accuracy.

The system is then melt-designed using these new values. This procedure is followed after the completion of certain key elements. At most, the last melt design will require a very tight central thickness tolerance on the last completed element. Since the now existing automatic lens design program on the IBM-7094 decreases the melt design computer time by a factor of 20, the above procedure requires only approximately one day for each melt design.

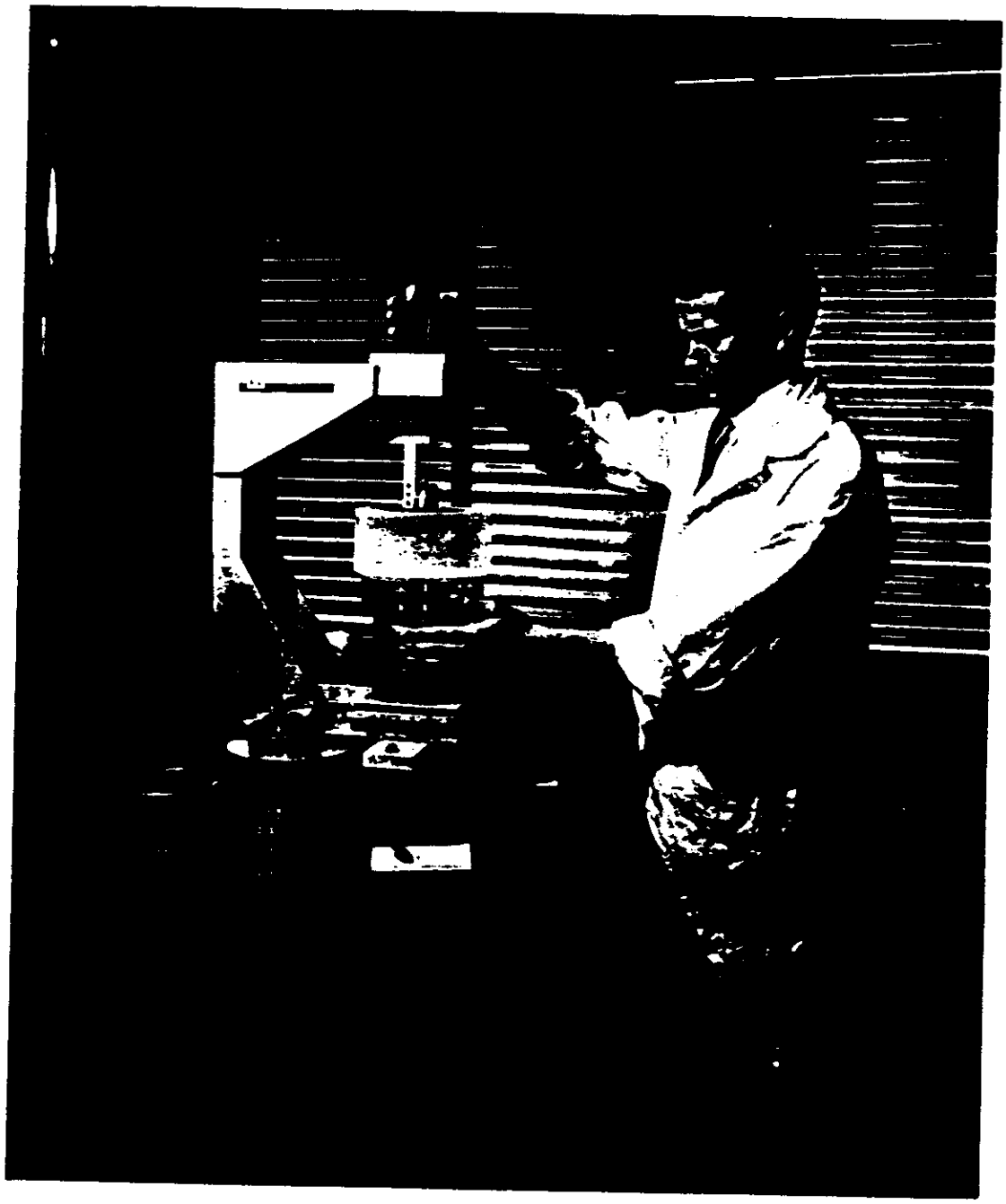

11,448

Fig. 2-9 — Special center-thickness measuring fixture

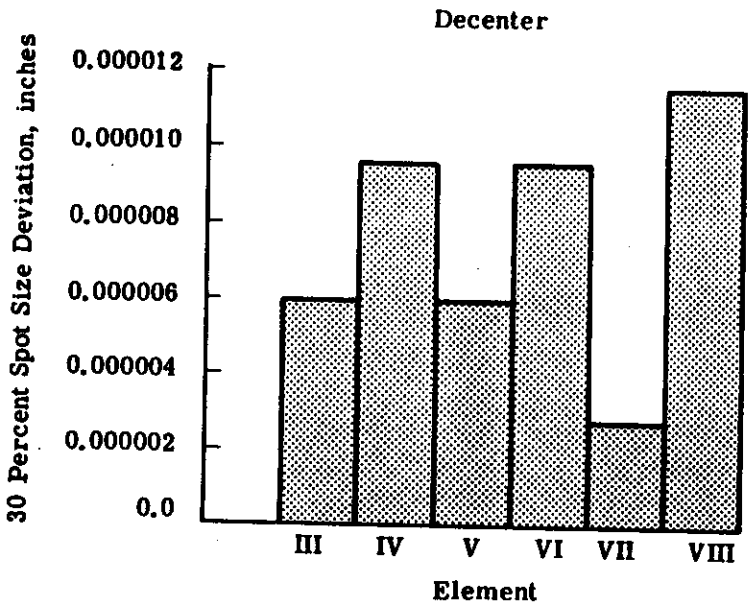

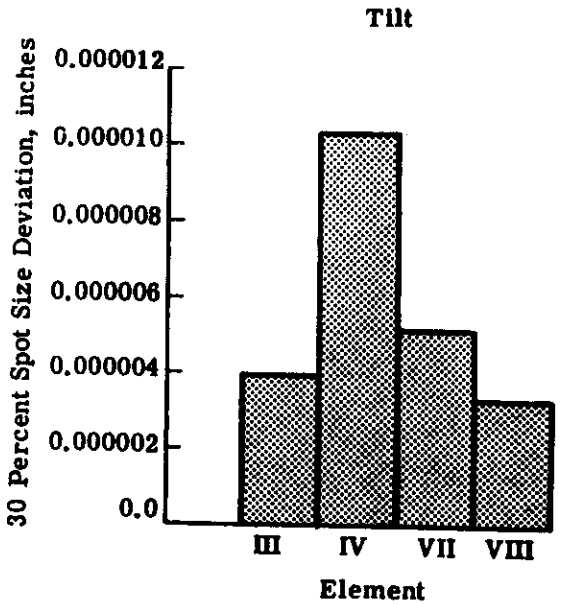

Fig. 2-10 — Image sensitivities relative to present measuring techniques (assuming 30-microinch gauge error and 25-microinch table run-out error)

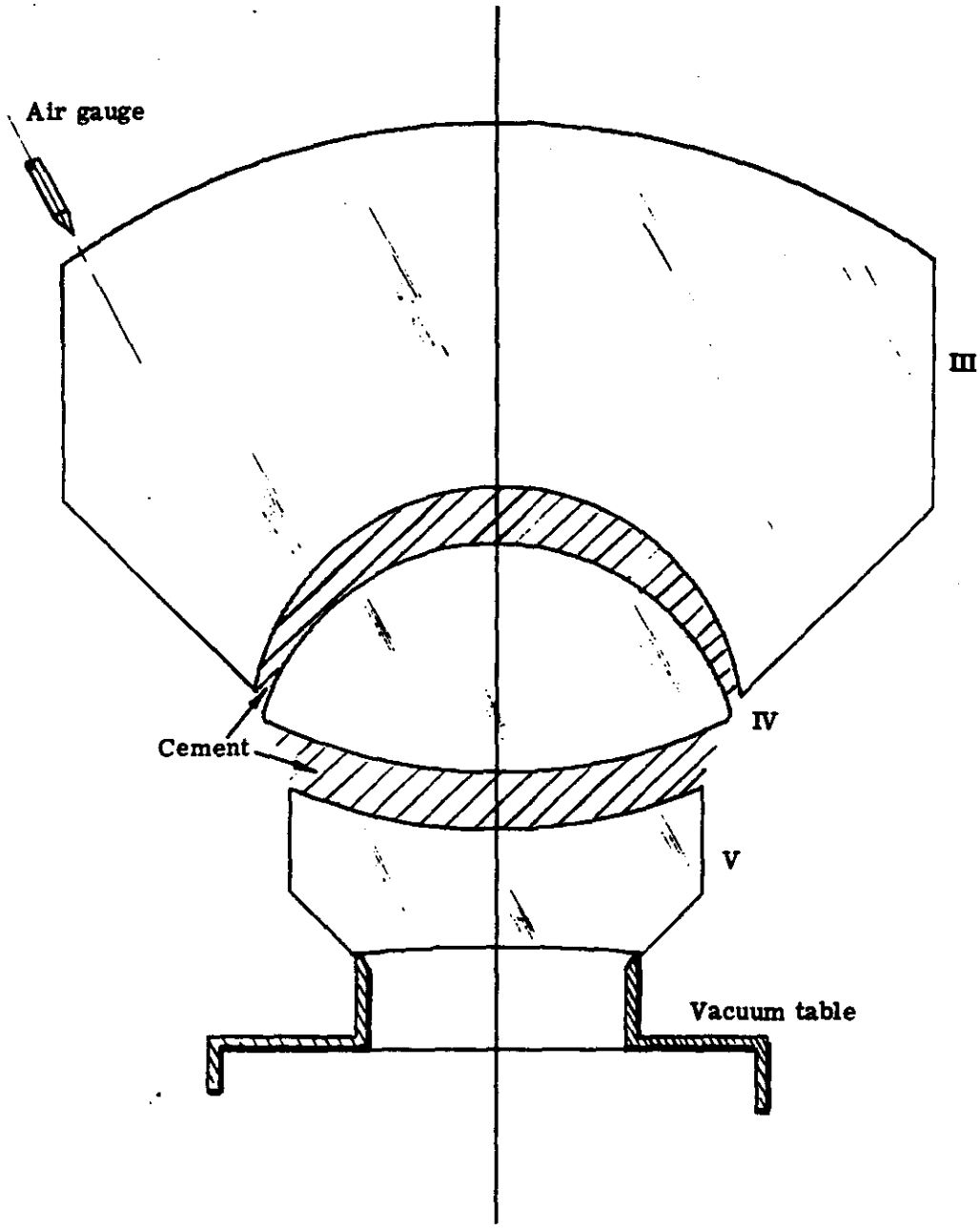

Fig. 2-11 — Positioning of triplet elements during cementing process (computer-generated drawing)

2. Element Fabrication

Test plate sets for all surfaces have been fabricated. The elements have been generated, and are presently in the polishing and figuring stages. Figure 2-12 illustrates the lens elements going through the various fabrication processes.

3. Aspheric Measuring Machine

The aspheric measuring machine (Figures 2-13, 2-14, and 2-15) is the measuring stick for the Itek optical shop personnel who hand-figure the aspheric elements to better than the 1λ (20×10^{-6} inch) tolerance set by the optical design. This machine is an automatic x–z coordinate measuring device which measures the profile of the aspheric surface.

An x–z coordinate tabulation will be generated for each aspheric by the optical designer. These coordinates will be punched onto paper tape for input into the machine. The paper tape reader will drive the x-leadscrew by fixed controllable increments. A servo device will drive the z-coordinate drum micrometer until the electronic pick-up on the micrometer tip has reached a null position. At that time, a 2000-count-per-turn angular encoder connected to the micrometer shaft will input its count into a recorder. The actual z-coordinate measured, and the correct z-coordinate as read from the punched paper tape will then be compared, and the difference automatically plotted out on a recorder. The tape reader will advance to the next set of coordinates, and the second point will be plotted, and so on until the whole aspheric contour has been established.

Present error analysis shows that the machine will measure accurately to better than 10×10^{-6} inch. Absolute calibration can be obtained against known optical flats or spheres when the device becomes fully operative. Optical tolerance analysis indicates that this degree of measuring accuracy should be entirely adequate for the production of the central aspherics.

Calibration of this machine against a known flat shows that the horizontal slide humps 70 microinches across a $3\frac{1}{2}$-inch diameter test flat. However, this error is reproducible to 8 microinches, and can be corrected by altering the input tape accordingly.

The final electronic input and output devices are presently being tested and debugged.

4. Cementing

Itek's present edging equipment allows elements to be edged round with a total indicator run-out error of only 40×10^{-6} inch, and the mounting flats can be ground relative to the polished surfaces of the elements to better than 1 second of arc. The final optical tolerance analysis indicates that this will be sufficiently accurate to allow edge centering in the cementing operation.

A set of cementing jigs and fixtures have been designed and are presently being built to facilitate the alignment of the elements as they are cemented. These fixtures will be attached to the Trans-o-Round roundness checker which will be used to actually make the alignment.

The fixtures will basically consist of a set of nested tubular rings containing differential adjusting screws as shown in Figure 2-16. The differential screw will be used to obtain very fine control in the alignment process.

The bottom element (Number 5) will be aligned using the roundness checker with two electronic gauges (one for the top surface and one for the edge) and a dual channel recorder. The top element (Number 4) would then be placed in position, the gauges would be removed from the bottom element and placed on the edge and top surface of the top element (see Figure 2-9).

Polishing process

Final figuring process

Examining lens element for visible imperfections

Making a test plate match

Fig. 2-12 — Element fabrication

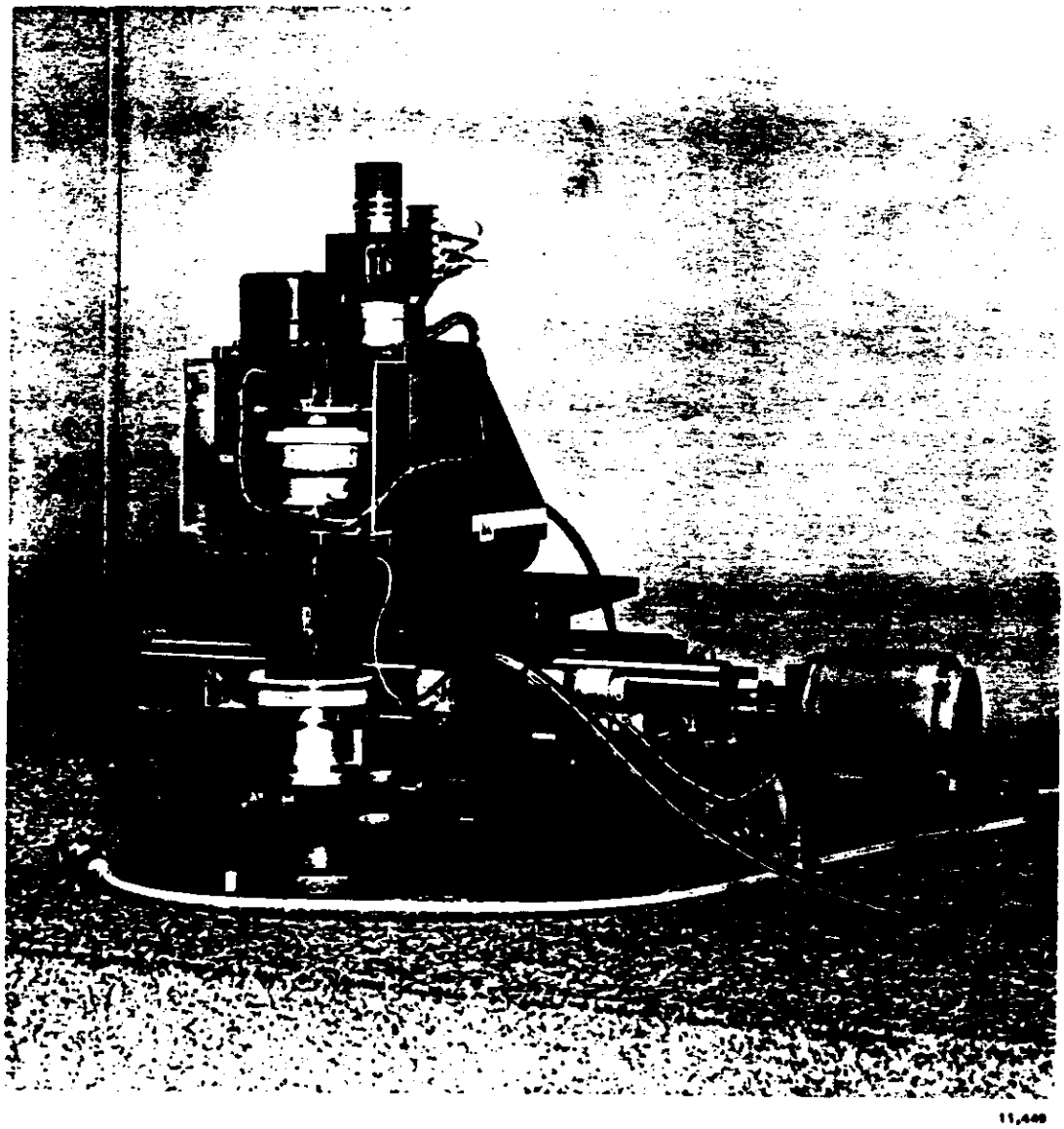

11,440

Fig. 2-13 — Aspheric measuring machine

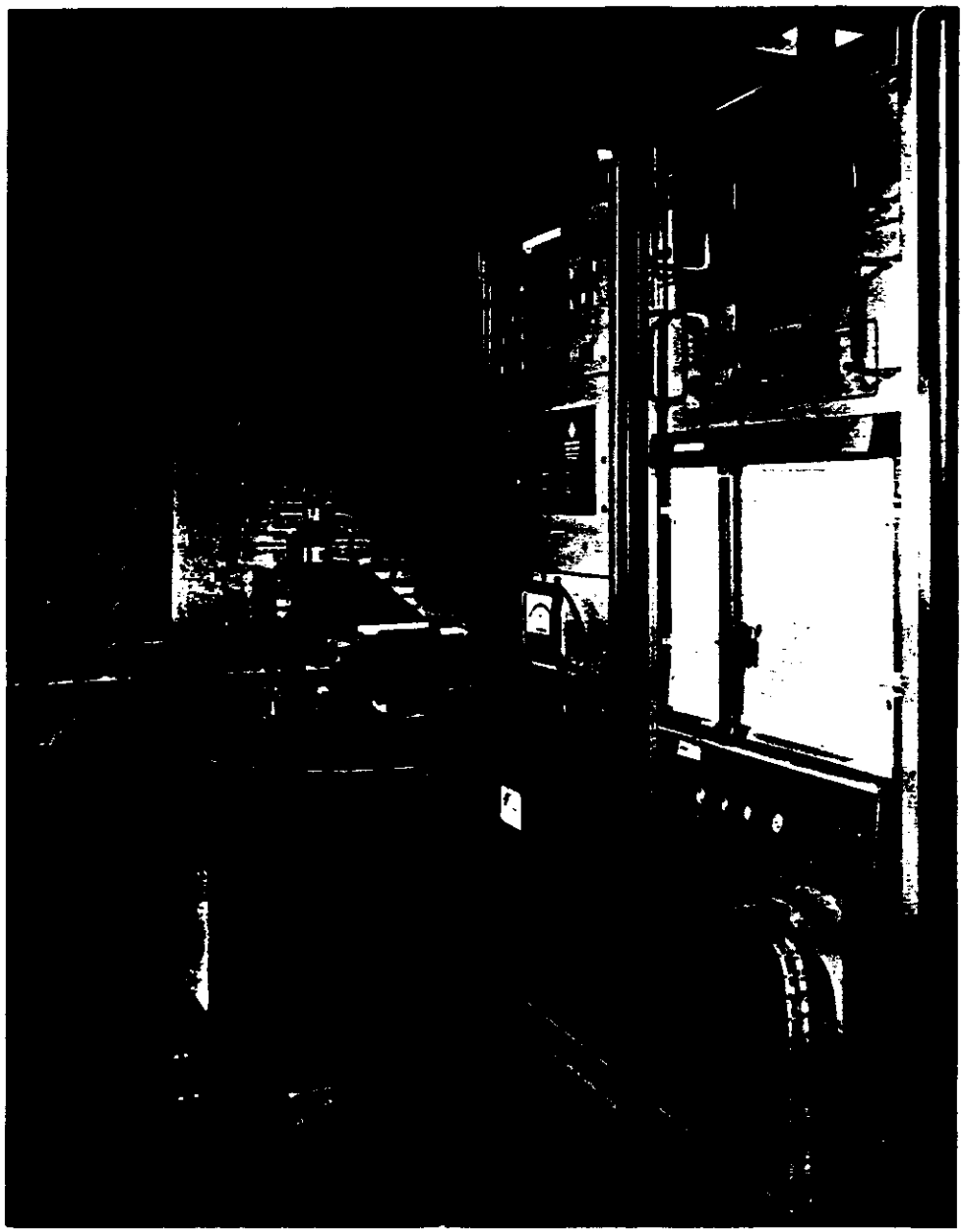

11,447

Fig. 2-14 — Aspheric measuring machine, overall setup

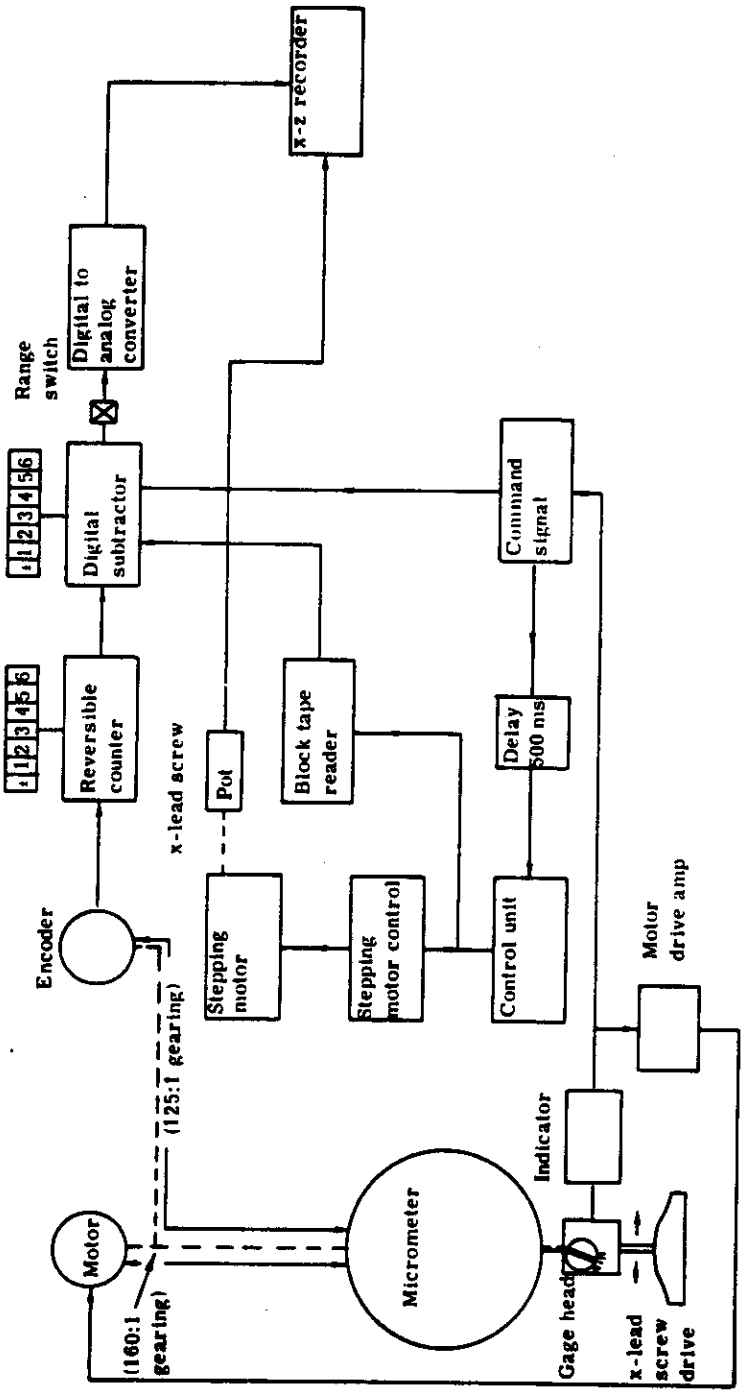

Fig. 2-15 — Aspheric measuring machine, servo block diagram